5-2011

Canal Wave Oscillation Phenomena Due to Column Vortex Shedding

Adam M. Howes
Utah State University

CANAL WAVE OSCILLATION PHENOMENA DUE TO COLUMN VORTEX SHEDDING

by

Adam M. Howes

A thesis submitted in partial fulfillment
of the requirements for the degree

of

MASTER OF SCIENCE

in

Civil and Environmental Engineering

Approved:

Steven L. Barfuss Major Professor	William J. Rahmeyer Committee Member
Joseph A. Caliendo Committee Member	Byron R. Burnham Dean of Graduate Studies

UTAH STATE UNIVERSITY
Logan, Utah

2011

ABSTRACT

Canal Wave Oscillation Phenomena Due to Column Vortex Shedding

by

Adam M. Howes, Master of Science

Utah State University, 2011

Major Professor: Steven L. Barfuss
Department: Civil and Environmental Engineering

The GARVEE Transportation Program started by the Idaho Transportation Department has improved parts of I-84 in Boise, Idaho. These desired improvements led to the widening of a bridge over the New York Canal (NYC) in 2009. To support the wider road, additional bridge columns were installed. The new bridge columns had a larger diameter than the existing columns and raised the number of columns from 28 to 60.

Construction was completed just before the irrigation season began. During the first irrigation season it was observed that waves and oscillations were occurring within the canal immediately adjacent to the bridge structure. Throughout the irrigation season, it was observed that the intensity of the oscillations would vary. It was also observed that the wave oscillations propagated upstream and downstream from the bridge structure. Both longitudinal and transverse waves were observed. The waves appeared to originate in the section of the canal that was under the I-84 Bridge.

A physical model was built in 2010 at Utah State University's (USU) Utah Water Research Laboratory (UWRL) in an attempt to simulate the oscillation phenomenon and to develop potential solutions to the problem. During the original modeling work, a thorough investigation to the causes of this phenomenon was not accomplished due to time constraints. The objective of the follow-up research presented in this thesis was to qualitatively determine the causes of the oscillations. Laboratory tests were performed using the original physical model used in the original 2010 testing.

(63 pages)

CONTENTS

LIST OF TABLES

LIST OF FIGURES

LIST OF ABBREVIATIONS

NYC	New York Canal
OD	Outer Diameter
USU	Utah State University
USBR	United States Bureau of Reclamation
UWRL	Utah Water Research Laboratory
WS	Water Surface

CHAPTER I

INTRODUCTION

In early 2009 the I-84 bridge expansion over the New York Canal (NYC) was completed. During the irrigation season following the completion of the bridge it was observed that there were wave oscillations present. The intensity of these oscillations varied throughout the season but caused concern because of the erosion these oscillations caused. The exact location of the oscillation's origin was not certain but both longitudinal and transverse waves were being generated.

In 1967 a similar oscillation phenomena occurred in the Delta Mendota Canal (Schuster 1967). This canal also experienced vertical waves which seemed to be generated by the bridge piers. The USBR decided to build a physical model to study the waves and to find a solution to the problem. From the physical model test results it was decided that a full closure of the pier segments was necessary to minimize the wave heights (Schuster 1967).

Similar to the case of the Delta Mendota Canal, a physical model study was proposed in order to get a better understanding of the wave oscillation phenomenon in the NYC canal. USU's UWRL was given the task of constructing a physical model. The purpose of the model study was first to recreate the oscillations and then to find potential solutions to the problem. Time and funding did not permit the UWRL's engineering team to investigate the cause of the oscillating waves.

During physical model tests, it was observed that the oscillations could be recreated at the same hydraulic conditions as the prototype. The engineering team had to

begin finding probable causes for the oscillation phenomenon before they could focus on finding potential solutions. Upstream canal flow conditions were distorted in an effort to increase or to reduce the oscillations. In doing so it was determined that upstream canal flow conditions did have an effect upon the oscillations. In addition, surface conditions were distorted which also had an effect upon the oscillations. Upstream and downstream canal bends in the prototype were initially thought to be a potential cause for the oscillations, yet since the physical model was able to replicate the oscillations without the upstream and downstream bends it was determined that those bends did not have an effect upon the oscillations (Rahmeyer et al. 2010). The irrigation turnouts on both the upstream and downstream ends of the I-84 bridge were also covered and it was determined that they did not have an effect upon the oscillations. The 32 new columns were then removed leaving the original 28 columns. This configuration was tested to see if the oscillation phenomenon was related to the original column configuration or was due to the new columns. It was observed that negligible oscillations occurred because of these original columns (Rahmeyer et al. 2010).

The asymmetry of the right and left rows of columns were also thought to be a concern. The asymmetry was measured by the angle of a line between the two upstream piers and the center line of the canal. Asymmetry decreases between the rows of piers when this angle is closer to 90 degrees. This angle in the Delta Mendota Canal (Figure A13) was much further from 90 degrees than was measured in the NYC canal (Figure A10). Because oscillations occurred regardless of the amount of asymmetry in both cases this topic was not researched further.

Flow conditions in the canal were found to be caused by various interactions between the water and boundaries which generated many potential causes in the oscillations.

- Subcritical flow exists in the entire canal section being tested.
- Upstream conditions of the flow are steady and uniform.
- Pier interaction with the flow creates a phenomenon known as vortex shedding.
- Vortex shedding has been found to be the producer of transverse and longitudinal waves (Zima and Ackerman 2002).

Rahmeyer et al. 2010 summarizes the wave oscillation phenomena by giving some important observations.

- Upstream canal distortions reduce the oscillations
- Water surface (WS) disturbances effect the oscillations
- Oscillations only occurred at uniform and steady flows
- Oscillations moved a significant distance upstream and downstream from the I-84 Bridge in the prototype
- There was an increase in flow depth in the center passage region of the canal between the two rows of columns that would be followed by a decrease in flow depth. During the decrease in flow depth there was cross flow from the center passage region to the outer passage regions (the area between the column rows and the sloping walls).

Several solutions to stop the oscillations were tested by Rahmeyer et al. (2010) and are shown in Figure A6. These included fully encapsulating each row of columns,

encapsulating every other two columns in each row, adding a column tail, and attaching a nose cone to the upstream face of select columns. The best solution found was the nose cones. This was a cost effective solution which would minimize the oscillations.

The precise mechanism which caused the oscillations to take place was never found during the initial model study. However, Rahmeyer et al. (2010) make some assumptions and hypothesizes a few potential causes.

- Vortex generation of columns combine to create a wake or train of vortices that reduce flow in the center passage. This effect causes a buildup of volume in the center passage region which then cross-flows into the outer regions, thus creating the oscillations.
- The longitudinal columns asymmetry
- Differences in hydraulic radii from the outer passages and center passage.

As previously mentioned oscillation phenomena was also investigated by Zima and Ackerman in 2002. Their studies looked at the effects of spacing upon oscillations as well as various column configurations. Their work showed the relationship between oscillations and vortex shedding. Their set up was not similar enough to match the configuration of the NYC canal, so a model study was still justified. Despite their differences in the physical model set up, many of their ideas and findings were consistent with this study.

The research done in this thesis explores potential generators of this phenomenon by testing various configurations through additional physical model testing. Research was done in a qualitative fashion to better understand the problem and test more configurations than would have been allowed if a quantitative analysis were done.

Observations of patterns within the data and observations of flow conditions physically seen in the model were key to the success of this research. Subsequent sections in this thesis compare amplitudes of the vertical wave height and the frequency of the oscillations. Results given in this document indicate whether a configuration increases, decreases, or does not change these values when compared to a base value. Chapter II looks into changing the canal geometry in the I-84 bridge section to having vertical walls instead of sloping side-walls. It also considered the effects of changing the angle of the columns to the walls. Chapter III looks into column spacing and its effects upon the oscillation phenomenon. All of these tests were performed in the same physical model used for the testing done by Rahmeyer et al. All of the results in the subsequent sections are reported with flow being quantified by prototype cfs so as to be comparative to the results from Rahmeyer et al. All other results are reported in model units.

CHAPTER II

VERTICAL WALLS

ABSTRACT

Oscillations in the physical model built by Rahmeyer et al. (2010) successfully modeled the oscillations found in the prototype. It is believed that there are several reasons that these oscillations take place. One potential cause for the increased magnitude of the waves was the trapezoidal shape of the canal. The sloped sides of the trapezoidal cross section were thought to make it easier for the transverse oscillations to gain strength and amplitude.

Vertical plywood walls were installed to simulate a rectangular cross section as compared to the existing trapezoidal shape of the canal. The vertical walls were found to dampen the oscillations at lower flows and depths but overall caused larger amplitude oscillations at an increased frequency at higher depths and flows.

The angle between the columns and the walls (in plan view) also had an effect upon the amplitude of the oscillations. When the walls were parallel to the column rows the vertical wave height was significantly decreased compared to the original vertical wall orientation, but they had the same frequency. When the angle between the columns and walls was increased by 1 degree from the original configurations angle, the wave-height amplitude was less than the amplitude of the original configuration, but it had the same frequency. Qualitatively, it was determined that the angle between the columns and the walls had an effect upon the oscillation phenomenon.

INTRODUCTION

Little information was found for the cause of the oscillation phenomenon in the NYC in the original testing (Rahmeyer et al. 2010). Several factors may be at work to cause these oscillations to occur and to have the amplitude that they do. The trapezoidal geometry was believed to increase the amplitude of the oscillations in the model. Thought was given to modifying the model in such a way to keep the cross sectional area and the depth consistent with the trapezoidal channel. This would have entailed major model modifications and was thus not done. It was decided that testing certain velocities was more important than having the depth and area consistent. Approach walls were installed at the toe of the left and right trapezoidal walls to convey more of the flow into the vertical section of the model (Figure A7). For documentation purposes, the terms left and right are used when describing the columns or the canal, the point of reference is taken from an upstream looking downstream viewpoint. The vertical walls were tested with and without approach walls.

Another factor that was thought to cause the oscillation phenomenon was the angle of the columns to the walls. The angle from the columns to the walls was about 0.7 degrees in the original set up. This angle was set to zero degrees and was then increased by one degree to create two separate set-ups. Angle changes were set-up by rotating the vertical walls until the angle between the walls and the columns were zero or 1.7 degrees.

EXPERIMENTAL PROCEDURE

At the Utah Water Research Laboratory in Logan, Utah a model of the NYC canal was constructed. It was built based on Froude similitude at a 1:9 scale. The 1:9 scale was chosen to optimize the model's abilities to replicate the oscillation phenomena (Rahmeyer et al. 2010) and was as large of a model that was feasible in the laboratory. The model was built to match the NYC's topography and roughness in order to simulate the prototype. The construction of the model included building 430 prototype ft of canal topography upstream of the I-84 bridge, and 230 prototype ft of canal topography downstream of the I-84 bridge using gravel with mortar to prevent sediment movement (Rahmeyer et al. 2010). Figure A1 is a schematic of the physical model and Figure A3 shows the upstream topography. The I-84 Bridge crossing section was constructed with painted plywood on the invert and the sides to model the concrete lining of the prototype. 60 columns were constructed from smooth PVC pipes and were machined to the proper diameters to match the original columns and those installed as part of the I-84 widening process. Figure A2 shows the model's I-84 bridge crossing including the columns in the canal. There were 28 original columns with an outer diameter (OD) of 24.29 prototype inches, and 32 new columns with an OD of 28.17 inches (Rahmeyer et al. 2010). Each column was given a name associated with it depending on its location and is shown in Figure A10. Upstream and downstream irrigation turnouts and the support for the Wright Street Bridge were also part of the physical model. Figure A4 shows the Wright Street Bridge pier. Since the model is only a section of a very long canal it was necessary to install stop logs as shown in Figure A5. Because the flow regime in the canal was

subcritical these stop logs were necessary to back up the flow to the desired depth (Rahmeyer et al. 2010).

Water was supplied to the model from First Dam in Logan Utah and was conveyed to the model through a series of pipes. The pipes fed into a head box shown in Figure A1. This helped to dissipate the energy of the water exiting the pipe. Steel mesh and nylon netting material were used to further dissipate the energy of the water entering the model to make the flow uniform and the WS as calm as possible (Figure A8). The flow rate was measured using a calibrated 20-inch venturi meter. Oscillation frequencies were measured using a stopwatch. A ruler was used to measure both vertical and wall wave heights. The depth was measured using a point gauge installed on the upstream end of the bridge section as shown in Figure A9. The location of the maximum wave location was taken from an arbitrary datum which was instrumental in the construction process. Each of the distances from the datum reported in Appendix B are measurements of the distance downstream from the datum.

The depth of the flow was controlled by the downstream stop logs and the flow rate was controlled using a 20-inch butterfly valve. A series of flow rates and depths were tested for each model configuration. Each setup of depth and flow was given ample time to stabilize to ensure that the oscillations had time to develop. Model runs were set for a minimum of 60 to 90 prototype minutes which through Froude scaling converts to 20-30 model minutes (Rahmeyer et al. 2010).

Velocity measurements were taken at the upstream and downstream ends of the vertical section at a flow rate of 2000 prototype cfs for each run. This was done to find the upstream and downstream velocity profiles for each of the various runs. In the tables

the terms “FL” and “FR” are abbreviations for “far left” and “far right” respectively. They are the velocity measurements taken on the opposite side of the vertical walls to find the amount of flow passing on the outside of the vertical walls.

Vertical walls were constructed out of ¾-inch plywood and were installed at the toe of the right and left sides of the trapezoidal bridge section. Since the surface roughness of the canal did not show an effect upon the oscillations (Rahmeyer et al. 2010), the vertical walls were not painted. When the angle of the vertical wall to the columns was changed they were rotated by keeping one end of the vertical wall at the toe of the trapezoidal side while the other end was adjusted to match the desired angle change as is shown in Figure A12.

Approach walls were installed, as shown in Figure A7, on the upstream end of the vertical section. The purpose of the approach walls was to convey the bulk of the flow into the rectangular section. A series of tests was performed to find the worst case scenario for the vertical wall configuration. Depths of 11, 12, and 13 model inches were tested at a range of flow rates varying from 1800 to 3150 prototype cfs. The minimum depth of 11 in model was chosen because the original model testing found the maximum oscillations at a depth of 11.125 model inches at a flow rate of 2066 cfs prototype (Rahmeyer et al. 2010). The maximum depth of 13 inches was chosen because the columns would be submerged above this depth. Finally the 12 inches model depth was chosen to test a wider range of possible maximum oscillations.

RESULTS AND ANALYSIS

With approach walls. Results from these tests are displayed in Tables B4, B5, and B6. It was found that the magnitudes of the oscillations increased from those reported by Rahmeyer et al. during the original model study. The 11, 12, and 13 model inch depth runs had a maximum oscillation of 1.38, 1.44, and 1.88 model inches, respectively. As depth increased so did the amplitude of the oscillations. The maximum amplitudes occurred at different flow rates for each depth. This corresponds to the velocity differences between varied flow rates and depths.

Table B13 shows the velocity calculations of the flow in the vertical section assuming it acts as a rectangular cross section (neglecting the flow outside the vertical wall section) with a base width of 92 model inches at various depths. The highlighted flow rates are those where the maximum oscillations occur. For this configuration the maximum oscillations occur at about 1.4 fps.

The frequency of the oscillations found by Rahmeyer et al. was 2.2 model seconds per cycle. This was increased after the installation of the approach walls to 1.6 model seconds per cycle. This difference can be attributed to distance of the walls to the columns being decreased which shortens the time to reflection of the oscillations from the walls and thus decreases the time per each cycle.

Without approach walls. The first series of tests done were to compare the results from original model testing when they reported the largest oscillations (Rahmeyer et al. 2010). Tables B1 and B2 compare the original data with the data from the vertical walls without approach walls configuration. It was decided to compare the data from Rahmeyer et al. without the approach walls so the velocity in the vertical section would

be as close to the same as the velocities in the trapezoidal tests. Table B3 shows the velocities taken from the original testing and compares it to the vertical wall tests (Rahmeyer et al. 2010). It is observed that the velocities are essentially the same with negligible variation. In the original research the maximum amplitude of the oscillations was 0.875 model inches at a flow rate and depth of 2066 cfs prototype and 11.5 in. model respectively (Table A1). With the vertical walls and no approach walls installed the amplitude of the oscillations was decreased significantly. The maximum amplitude of the vertical wall configuration in this series of tests was 0.125 model inches which occurred at several flow rates, including 2066 cfs prototype, and is shown in Tables B1 and B2.

The largest oscillations which were found with the approach walls installed, occurred at a depth of 13 inches. This same depth was tested without the approach walls to see what the maximum oscillation would be compared to the no approach wall results. Table B7 shows the maximum oscillation of 2.38 model inches occurring at 3300 cfs prototype. At this flow rate the velocity is calculated to be 1.35 fps, assuming a trapezoidal geometry (Table B14). This is consistent with the maximum oscillations found with the approach walls, which also occurred around 1.4 fps. The frequency of the oscillations was also found to be consistent with the approach wall data. Original testing observed a bulking of flow in the center passage followed by an outflow to the outer passages (Rahmeyer et al. 2010). This same observation was made here but was much more obvious to an observer because of the large amplitude of the oscillations.

Nose cones were installed at a flow rate of 3300 prototype cfs and 13 model inches, which was the worst condition for oscillations found for this configuration. This

was done to see if they would dissipate even larger magnitude oscillations than they were originally tested for. They performed as they were observed and reported to perform in their initial testing (Rahmeyer et al. 2010). Despite the amplitude of the oscillations being much higher than was found without approach walls, the nose cones eliminated the oscillations.

Oscillatory behavior should theoretically be consistent in the vertical wall tests with or without the approach walls when the same velocity is observed in the vertical section. An inconsistency in the data was found when comparing the magnitudes from the vertical wall configurations with approach walls to those tests done without them. The reason for the inconsistency is the flow separation which occurred at the upstream end of the vertical section when the approach walls were installed. This separation caused increased turbulence and eddy generation which may have conflicted with the turbulence and eddy generation of the columns, especially those on the upstream end of the vertical section. Turbulence, eddy, and vortex generation of the columns must therefore be a major component for the oscillation generation.

Angle from wall to column decreased to 0º. The angles between the column rows and the toes of the trapezoidal channel are eschewed. From topographic data given it was determined that the angle between the toes of the channel and the rows of columns was about 0.7º and is shown in Figure A12. This angle could be another potential cause for the oscillations. To see if the angle made a significant effect on the oscillations it was first tested at a zero degree angle as shown in Figure A12. Table B8 shows the results of these tests. Approach walls were not installed for the angle change tests to keep flow separation to a minimum. The maximum vertical wave height still occurred at 3300 cfs,

but the magnitude decreased from 2.38 model inches to 1.0 model inch. The frequency of the oscillations remains relatively the same. This decrease in amplitude was not large enough to give too much credence to the idea that the angle of the columns to the wall is a large contributor to the oscillation development process, although it is still seen to be a contributor. Rows of piers in the Delta Mendota Canal appear to be parallel to the trapezoidal toes as shown in Figure A13, yet the oscillations still occurred (Schuster 1967). This fact gives further credibility to the findings that a parallel relationship between canal walls and pier rows does not eliminate the oscillations. Accordingly, it may be concluded that the angle of the rows of piers in relation to the vertical side walls of the canal is not a large contributing factor to the oscillation phenomenon.

Angle from wall to columns increased by 1º. In an effort to determine the effects of the angle upon the oscillation, the angle was then increased as shown in Figure A12 as an inverse relationship test. Results from this test, displayed in Table B9, show that the maximum oscillation occurs at 3300 prototype cfs and a depth of 13 model inches. That is the same flow rate and depth where the maximum wave heights were found for the zero degree and the original angle configurations. The amplitude of these waves is higher than the waves of the zero-degree configuration, but lower than waves of the original angle configuration.

APPLICATION

Further research should be done to create a more broad and accurate range of recommendations for consideration when designing the geometry and pier configuration of a canal passing under a bridge. Recommendations given here are generalized for the

findings done on a few sets of column and canal geometries. Cross sectional shape of the canal has been found to have an impact upon wave generation. When low velocities are expected in the canal at moderate depths a rectangular cross section has been found to be more efficient at oscillation dissipation. At higher depths and velocities trapezoidal canal geometry is more efficient.

The angle which rows of columns or piers has to the walls played a minimal part in the oscillation generation. Angles to the wall may be controlled by the structural requirements of the bridge and/or the foundation upon which they rest. When designing piers to be placed in an operational canal it is recommended that the rows of piers be parallel to the canal walls if design restraints allow.

CONCLUSIONS

The amplitude of the oscillations which occur with the vertical walls was lower than the amplitude of the oscillations found in the original testing at low flows with their corresponding depths (Rahmeyer et al. 2010). However, at higher flows the vertical walls experience significantly larger oscillations than were found by in the original data (Rahmeyer et al. 2010). The changes in frequency and amplitude can be attributed to the geometry change from trapezoidal to rectangular cross section and/or the closer proximity of the walls to the columns.

The angle of the columns to the walls has been shown to have an effect upon the oscillations, see Figure A12. When the columns were parallel to the wall the oscillations were decreased. Oscillations were also decreased when the angle was increased by one degree. The original angle configuration created the largest oscillations of the three

configurations. Wave formations occurred in the Delta Mendota Canal despite the rows of piers being parallel to the toe of the trapezoidal walls. Thus the angle of the row of piers to the wall is not a large driving force behind oscillation generation.

As was previously mentioned, the zero-degree configuration's amplitude change is significant enough to state that the angle change has an effect upon the oscillations, but its effect may not be paramount. Because of how these angle change configurations were installed it may have caused more turbulence and eddy formation on the upstream end of the vertical section. With the walls being put into the flow path on the upstream side turbulence may have increased. This may have caused the oscillations to dampen as was seen in the tests with the approach walls installed. Even with the flow being more turbulent on the upstream end of the vertical section in the approach wall tests, oscillations were still observed, but seemed to be dampened by that effect. This same dampening effect could potentially be the cause for the decrease in oscillation intensity. But, as was observed in the approach wall case, the angle change still had an effect upon the oscillations.

CHAPTER III

COLUMN SPACING

ABSTRACT

A physical model was built for the purpose of replicating the oscillation phenomena discovered in the New York Canal. The oscillations experienced in the NYC are believed to have several potential causes. Chapter II investigated the additional effects due to the canal's geometry upon the wave oscillations. It is believed that the columns are source significant contributor to the generation of these oscillations (Rahmeyer et al. 2010). The original column configuration was tested again in the trapezoidal canal, and a second configuration where every other column was removed was also tested. Dye and audio visual equipment was utilized to provide a qualitative view of the probable causes for the oscillations. Vortex shedding and column approach velocity were subsequently found to be large contributors to oscillation generation. The column nose cones that were developed during the original model tests provide further insight into the causes of the wave oscillations, by showing how the flow conditions change with and without the nose cones installed on the face of the columns.

INTRODUCTION

There is not much known about the subject of oscillations in open channel caused by canal obstructions. Numerous papers have been written upon vortex shedding around cylinders or oscillations due to vegetation, but few are applicable to this study. One case, however, is particularly applicable to this study. This case was discovered by the USBR in the Delta Mendota Canal (Schuster 1967). Oscillations occurred in this canal with

piers from an overhead bridge being the observed generators of these oscillations (Figure A13). Another study done by Zima and Ackerman looked at the effects that various column spacing and configurations had on wave generation in open channels (Zima and Ackerman 2002). Both studies by the USBR and Zima and Ackerman are applicable to this study.

To study the effects of column spacing on the NYC's physical model there were a few different tests set up. The first set of tests were performed with the original column configuration, both with and without nose cones. Secondly, every even numbered column was removed to test the effects of increasing the spacing (Figure A11). A camcorder was utilized to record the observations made by injecting dye into the model. The dye helps an observer see the direction and conditions of the flow and helps one visualize turbulence and eddy formation which may not be obvious without dye. The three flow rates and depths with the largest oscillations found by Rahmeyer et al. were tested for all configurations. The flow condition of 3000 prototype cfs at a depth of 13 model inches was also tested for all configurations, because it was one of the worst conditions found for the vertical wall without approach wall data.

EXPERIMENTAL PROCEDURE

The experimental set up and operation of the model was consistent with the experimental procedure reported in Chapter II. The vertical walls were removed and the trapezoidal cross section was tested. The only physical changes to the model were the installation of nosecones on some runs and the removal of the even numbered columns on other runs (Figure A11). To be consistent with the original testing, nose cones were

installed on the right and left rows on columns 1, 4, 7, 11, 16, 21, and 26 (Rahmeyer et al. 2010). When the columns were initially installed they were screwed to the canal's invert. Upon removal, these screw holes were sealed and the sealant was smoothed to keep the integrity of the canal's lining.

Observations were made by injecting dye both on the upstream and downstream ends of the model to find similarities and differences between the interactions of the columns and water. A camcorder was used to record these observations so the observer could review the observations in greater depth after the testing had been done. Different configurations and test setups could then be observed side by side during video playback to observe flow patterns more easily. During the dye testing, there were several locations where the dye was injected. These points of interest were:

- Upstream face of the column
- Downstream face of the column
- Halfway between the columns
- 1 column diameter away from the row of columns
- 2 column diameters away from the row of columns

The right row of columns was chosen for these dye observations.

RESULTS AND ANALYSIS

Original column spacing without nose cones. Dye injected on the upstream face of R1 was evenly dispersed to the right and left of the column. This showed the uniformity of the flow approaching the model and the absence of vortex and turbulent forces on this face. R1's downstream face had a dead zone where the dye would collect

and was slowly dispersed after the dye was no longer being added. Small amounts of turbulence were observed there along with reverse flow. The dead zone or stagnation was formed by the high impact velocity on the upstream face of R1, which sent the flow around the column at a higher velocity. The flow did not converge until approximately one diameter downstream of the column. Halfway between R1 and R2 there were intermittent instances where the dye injected there would reverse flow to the downstream face of R1. Vortex shedding was observed there and would send the dye to the right and left of R2.

Upstream columns R1-R3 along with downstream columns R26-R30 all had the same upstream and downstream dye effects. Upstream faces were strongly influenced by the previous columns vortex shedding. Flow would go to the right or the left of the column with no time spent splitting the dye to both sides. downstream faces of these columns did not have any dead zones like was observed on R1. Vortex shedding was well established and steady for each column. Dye injected halfway between the columns would go either to the right or the left of the downstream columns.

Dye injected one diameter to the right or left of the row of columns was also influenced by the columns. It would intermittently get drawn into the row of columns followed by it being pushed away from them. When the dye was injected 2 diameters away it was not strongly influenced by the rows of columns.

Testing done by Zima and Ackerman used a variable in their analysis called the frequency ratio. It is expressed in Equation 1 below.

$$\frac{f_s}{f} \tag{1}$$

The term "f_s" represents the frequency of vortex shedding from one side of the cylinder and "f" represents the frequency of the transverse waves. Because the ratio is a dimensionless term the units of f and f_s are not important as long as they are the same. Zima and Ackerman found that the greatest wave amplitude occurred when the frequency ratio was between 0.7 and 1.3 (Zima and Ackerman 2002). Table B15 shows the results of the original column configuration test (without nose cones). Grey rows in the table represent tests where dye was used. White rows represent tests performed to check and repeat the results found in the original testing. The columns on the far right represent the frequency ratio for certain columns. Frequency ratios range between 0.88 and 1.03 for these maximum oscillations which are within the range of values reported by Zima and Ackerman.

H.T. Falvey also made observations about the relationship between the frequency of the oscillations and the frequency of the vortex shedding. He noted that in the case studied by the USBR in the Delta Mendota Canal that resonant frequencies played a part in the oscillation formation. He stated that large amplitude waves can be formed when the resonant frequency of the space between the rows of piers and the canal bank match the frequency of the vortex shedding (Falvey 1980). His findings were supported by the results of this testing and the findings of Zima and Ackerman

Original column spacing with nose cones. Flow around the nose cone installed on column R1 was split evenly between the right and the left. This supports what was already mentioned above that the approach conditions are steady and uniform. A large dead zone was developed behind R1. It was observed that this happened because the nosecones pushed the flow further to the right and the left than it did before the nose

cones were installed. Pushing the flow further to the right and left caused the converging point of the flow to occur at about column R2 rather than 1 column diameter downstream from R1 as was observed previously. Reverse flow and mild turbulence occurred in this dead zone allowing the dye to slowly dissipate after the injection ceased. Because of the dead zone created by the nose cone on R1 the vortex shedding abilities of columns R1, R2 and R3 were crippled. The nose cones essentially created a conditions in which the vortex shedding on each of the columns was no longer steady.

Upstream faces of columns R3 and R4 showed the reformation of vortex shedding on the columns immediately upstream from them. This was indicated by the dye being directed either to the left or right of the column. There were short increments on the upstream face of column R3 where the flow would split evenly between the right and left sides of the column. This would occur in between the usual shifts to the left and the right. This shows the crippling effect that the nosecone on R1 had on the vortex shedding ability of R2 which in turn affected R3. Nose cone R4 exhibited vortex shedding on the upstream side, because the flow would switch from left to right around the tip of the nose.

Dye injected on the upstream face of the R26's nose cone was seen to switch from the right and then to the left. This switching suggested the reestablishment of vortex shedding on the columns previous to R26. Dye injected on the downstream face of R2 showed the presence of a dead zone and reverse flows. The extent of this dead zone was not as large as the one created by R1, but extended about one column diameter downstream. Upstream and downstream observations on columns R27 through R30 showed that these columns were also experiencing the vortex phenomena. Column R27 though, had a mild dead zone behind it that would shift slightly left or slightly right

depending on its own vortex shedding. This dead zone extended just under one column diameter behind R27.

The reestablishment of vortex shedding on columns further downstream from R1 suggests that the impact velocity on subsequent nose cones is decreased which limit their ability to create these vortex crippling dead zones and turbulence. Also the increase in spacing between nosecones also affects the vortex shedding ability of the columns which precede them. Turbulence and impact velocity seem to be the major contributors to vortex and oscillation suppression.

Every other column remaining. Preliminary tests on this configuration were done with the vertical walls installed. This was done because the largest oscillations with the original column configuration were found with the vertical walls installed, and this would magnify the oscillations so they could be more obvious to the observer. Three depths of 11, 12, and 13 model inches were tested at several flow rates ranging from 2000 to 3700 prototype cfs. This wide range of tests was performed to find the worst case scenario based upon knowledge gleaned from previous vertical wall testing. Results from these tests are shown in Tables B10, B11, and B12. The frequency of the oscillations remained constant with that found in the original column configuration. At higher flow rates, and thus higher velocities, surface waves became more prominent and therefore, no noticeable oscillations occurred. The surface waves were generated because of the higher impact velocity on the upstream face of the remaining odd numbered columns. An amplitude of 0.5 model inches was the largest amplitude found in these tests which occurred at a depth of 13 model inches and 3500 prototype cfs (Table B12). Upon the removal of the even numbered columns the magnitude of the oscillations dropped

significantly. Thus the spacing of the columns was found to be very important in the formation of the oscillations.

An in-depth analysis of the flow conditions using dye was also performed for this configuration and Table B16 gives these results. The shaded rows represent the runs which were tested with dye, while the white regions are repeats of the dye tests to verify their results.

During the dye testing column R1 behaved the same as it did during the tests of the original configuration without the nosecones. The dead zone on the downstream side of the column was the same size, extending about 1 column diameter downstream. When dye was injected halfway between R1 and R3 the dye would shift to the right and left and was obviously being affected by the vortex shedding of R1.

Dye injected on the upstream face of column R3 would shift to the right and the left. However it would occasionally dwell directly on the upstream face which would disperse the dye evenly on both sides for a short period of time. When the dye was injected at the downstream face of R3 there was a dead zone formed there which extended almost 1 column diameter downstream. The dead zone shifted to the left and the right with the vortex shedding of R3. The formation of a dead zone on the downstream face of R3 suggests that the impact velocity on R3 is higher in this configuration than the original configuration. This contributes to the increased turbulence and formation of dead zones which inhibit the strength and formation of vortex shedding. Columns R5, R27, and R29 all behaved like column R3 with the only difference being the dead zone on these extended only ½ column diameters downstream.

Flow to the right and the left of the row of columns was affected by this configuration. When injected one diameter away, the dye would be drawn into the columns and pushed away as the vortex shedding occurred. At a distance of 2 or 3 diameters to the right or the left the dye would show more turbulence than was seen doing the same tests with the original configuration.

Frequency ratios for columns R3 and R5 ranged from 0.93-0.97. Because these numbers were within the range of 0.7-1.3, these runs would be experiencing the largest wave amplitudes (Zima and Ackerman 2002).

As was seen in the dye tests on the original column configuration with nose cones, the turbulence and approach velocity contribute to the dissipation of the oscillations and the vortex shedding.

APPLICATION

Column spacing was found to have an effect upon the oscillations. This effect was manifest by the decrease in wave magnitude when every even numbered column was removed. Decreasing wave magnitude was attributed to increased turbulence and vortex shedding interference. If oscillations of transverse and longitudinal waves are discovered in a canal it is suggested that these oscillations be diminished by increasing the turbulence and vortex shedding interference within the pier section. This can be done in the design phase by increasing the distance between piers in a row. The worst conditions were seen when the distance between columns was 2-2 ½ column diameters. Conditions improved when that spacing was increased to about six column diameters (Figure A14). It can also be done after construction by installing nose cones or another device which

may direct more flow away from the piers and increase the turbulence in the pier section. Head loss associated with the installation of these nosecones wasn't calculated in the tests, but may be an important factor to consider before installing into a canal.

CONCLUSIONS

Column configuration and spacing is important and pertinent to the generation of the oscillation phenomena. Two column configurations were tested and it was found that the original column configuration, shown in Figure A10, experienced the largest wave oscillations. When the spacing was increased by removing the even numbered columns, shown in Figure A11, the vertical wave height was greatly reduced. Thus oscillations are affected by the spacing of the columns.

Vortex generation is linked to the wave oscillations. When the frequency ratio is between the ranges of 0.7-1.3 the largest amplitude transverse waves should be produced (Zima and Ackerman 2002). This was found to be true in both configurations whose frequency ratios varied between the ranges of 0.88-1.03. This gives credence to the assumption that, given these different configurations, the maximum oscillations have been found.

Findings from the dye tests on the original configuration with nose cones and every other column removed show that turbulence and impact velocity play a role in oscillation formation. As the turbulence and impact velocity on individual piers was increased, the oscillations were decreased. Dead zone formation on the downstream face of columns and increased turbulence are products of the impact velocity on the upstream face of columns.

CHAPTER IV

SUMMARY AND CONCLUSIONS

A model study was performed to assess the potential causes for the oscillation phenomena discovered in the NYC Canal. Several potential causes were tested in the model to see what their effects upon the oscillations would be. Results found were more qualitative than quantitative. Conclusions for each of the configurations tested include recommended design guidelines for the prevention of oscillations.

Canal geometry and the orientation of rows of columns were tested to see what effect they had upon the oscillations. When various configurations of each were tested the oscillation dissipation was minimal. Because of this it is unlikely that these geometric configurations could be the main driving forces for the phenomena. The vertical walls decreased the water surface width which may have caused the increased amplitude of the oscillations. The effects of moving the vertical walls out to keep the same cross sectional area and depth in the prototype may change the amplitude of the oscillations. It is unknown whether this would increase or decrease the wave amplitude. The configuration tested did assist in dampening the oscillations, but when modified independently, the changes do not significantly reduce the oscillations.

Of the modeling configurations that were tested in this study, column spacing was found to have the greatest affect on the oscillation phenomenon. When the original configuration with nose cones was tested, it was noted that the nose cones directed the flow away from the rows of columns and created dead zones and generally increased turbulence. These dead zones decreased the vortex shedding near many of the columns

which were immediately downstream from them, but did not have a nose cone. Increasing the spacing between the columns was found to cause an increase in the velocity of the water impacting the upstream face of each of the columns. The higher impact velocity caused the flow to shed away from the row of columns similar to what was seen with the nose cones. The amount of turbulence was also increased in both cases.

Wave oscillations were found to be effected by the amount of turbulence and vortex shedding experienced by the columns. Frequency ratios in the column spacing tests ranged between 0.7 and 1.3 when the maximum oscillations were observed. This indicates that the frequency of the vortex shedding may be directly related to the magnitude of the oscillations (Zima and Ackerman 2002).

These guidelines are recommendations based on the research done in this thesis. These design guidelines should be utilized to prevent wave oscillations.

- At lower flows and depths, use a rectangular cross section with approach walls for the bridge section. This is because model tests showed a decrease in oscillation magnitude when comparing the rectangular and trapezoidal cross section tests at lower flows and depths.
- At higher flows and depths, use a trapezoidal cross section for the bridge section to minimize the oscillations. When comparing the rectangular and trapezoidal cross section tests at higher depths and flows, the trapezoidal cross section performed better at oscillation dampening than the rectangular cross section did.

- Set the angle of the column rows in relation to the wall or toe of the trapezoidal section to zero degrees. Model tests concluded that at zero degrees the oscillations were minimized compared to other angle configurations tested.
- Set the column spacing to six column diameters (Figure A14). This guideline is based upon the tests that were performed during this study. It may be possible to utilize a column spacing that is slightly less than six column diameters, but no testing was performed to verify this possibility.

Full enclosure of the space between the piers will remedy the problem (Schuster 1967 and Rahmeyer et al. 2010). Based on the research done in this thesis, the installation of nose cones or a device which will perform similarly may also remedy the problem. The nose cones increase the turbulence and direct the flow away from the columns which cause a dampening of the oscillations and vortex shedding. The nose cones should be designed so that they do not capture debris, they will not be damaged by debris impacting on them and they do not produce excess headloss through the bridge structure.

CHAPTER V

FUTURE RESEARCH

Due to time constraints the research was limited to observations based on a qualitative analysis. It is suggested that a more detailed study be performed to find the quantitative relationship between oscillations generation and column configuration. The relationship of resonance between the two rows of columns and oscillation generation could also be researched further. Along those same lines observations of the interaction of columns in a row with one another could potentially shed more understanding upon the subject. There are several column configurations which could also be tested to see what effects they have upon the flow conditions. These could include, but are not limited to:

- Changing the proximity of the columns to the walls
- Changing the asymmetry of the rows by moving one row further upstream or downstream
- Testing various column geometries and diameters

With increased knowledge about this unique wave oscillation phenomenon, designers should be able to avoid the problem.

REFERENCES

Falvey, H.T. (1980). "Bureau of Reclamation experiences with flow induced vibrations." *Practical experiences with flow induced vibrations*, E. Naudascher and D.Rockwell, eds., Springer, New York, 394.

Rahmeyer, W., Robison, E, and Barfuss, S.L. (2010). "Physical modeling of wave oscillations from the I-84 Bridge Crossing of the New York Canal in Boise, Idaho." *UWRL Report – USU 686*, Utah Water Res. Lab., Utah State University, Logan, Utah.

Schuster, J.C. (1967). "Canal capacity studies, Wave formation by bridge piers." *Hydraulics Branch Rep., HYD-485,* U.S. Bureau of Reclamation, Washington, D.C.

Zima, L., and Ackerman, A.L. (2002). "Wave Generation in Open channels by Vortex Shedding from Channel Obstructions." *J. Hyd. Engrg*, vol 128, 596-603.

APPENDICES

Appendix A: Figures and Photos

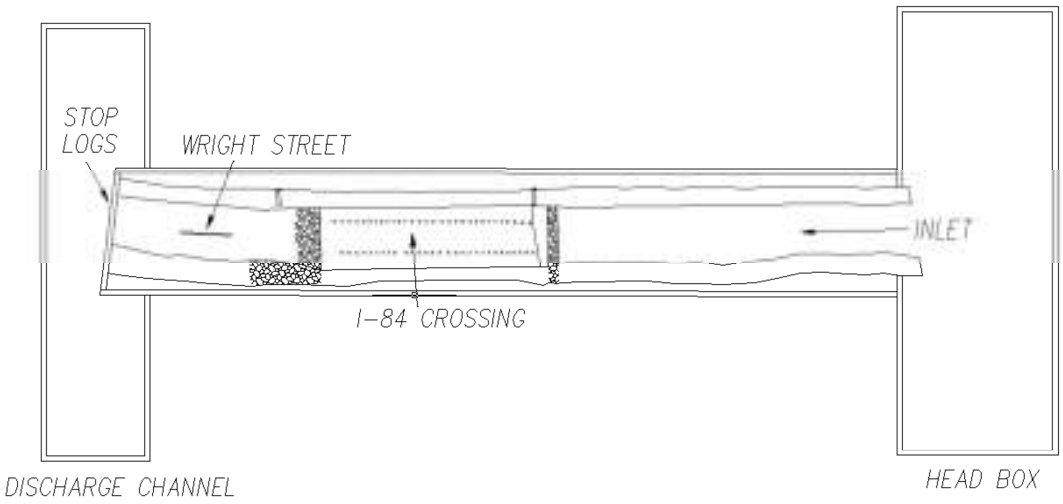

Figure A1. Physical model setup schematic including the I-84 crossing and the Wright Street Bridge. The flow direction is from right to left (Rahmeyer et al. 2010).

Figure A2. I-84 bridge crossing section looking downstream. Original columns are white and the new columns are black (Rahmeyer et al. 2010).

Figure A3. Upstream view of the canal with topography (Rahmeyer et al. 2010).

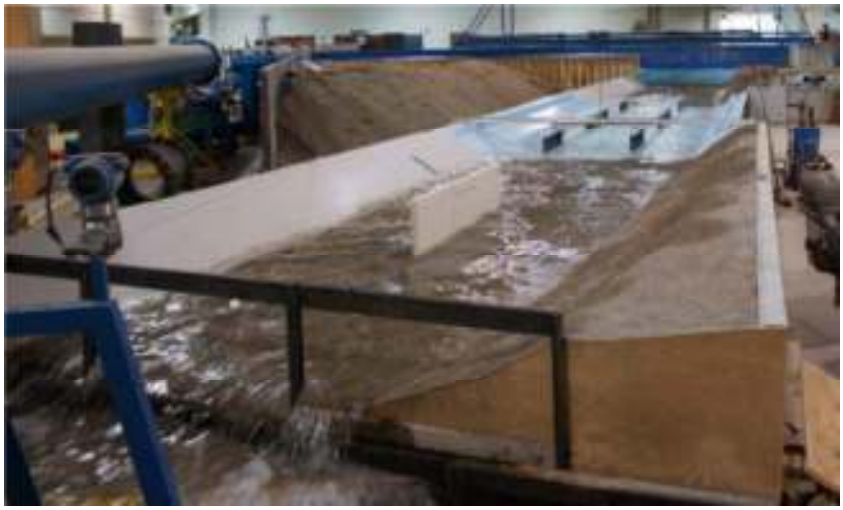

Figure A4. Upstream view of the entire model showing the Wright Street Bridge pier in white in the foreground (Rahmeyer et al. 2010).

Figure A5. Stop logs installed on the downstream end of the model to set flow depths (Rahmeyer et al. 2010).

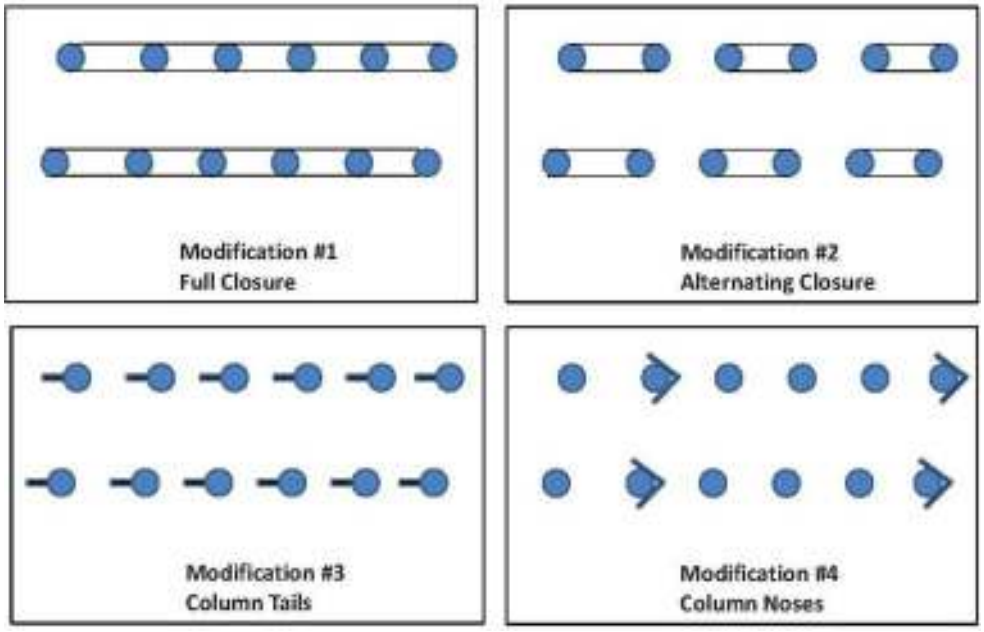

Figure A6. Column modifications tested to minimize the oscillation phenomena (Rahmeyer et al. 2010). Flow direction is from right to left.

Figure A7. Downstream view of the vertical section with the approach walls installed.

Figure A8. Upstream view of baffles which helped control approach conditions into the model.

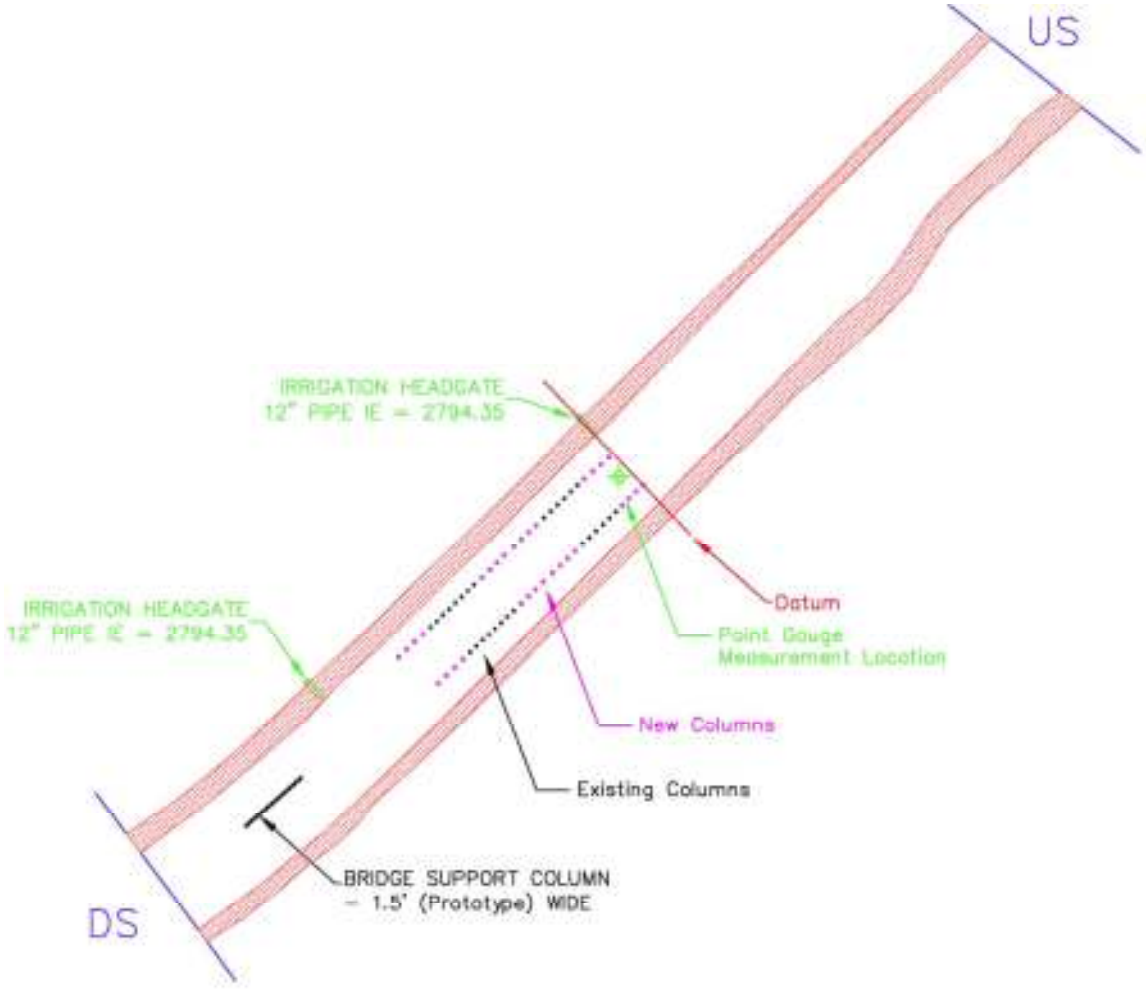

Figure A9. Plan view drawing of the model including the datum and point gauge location.

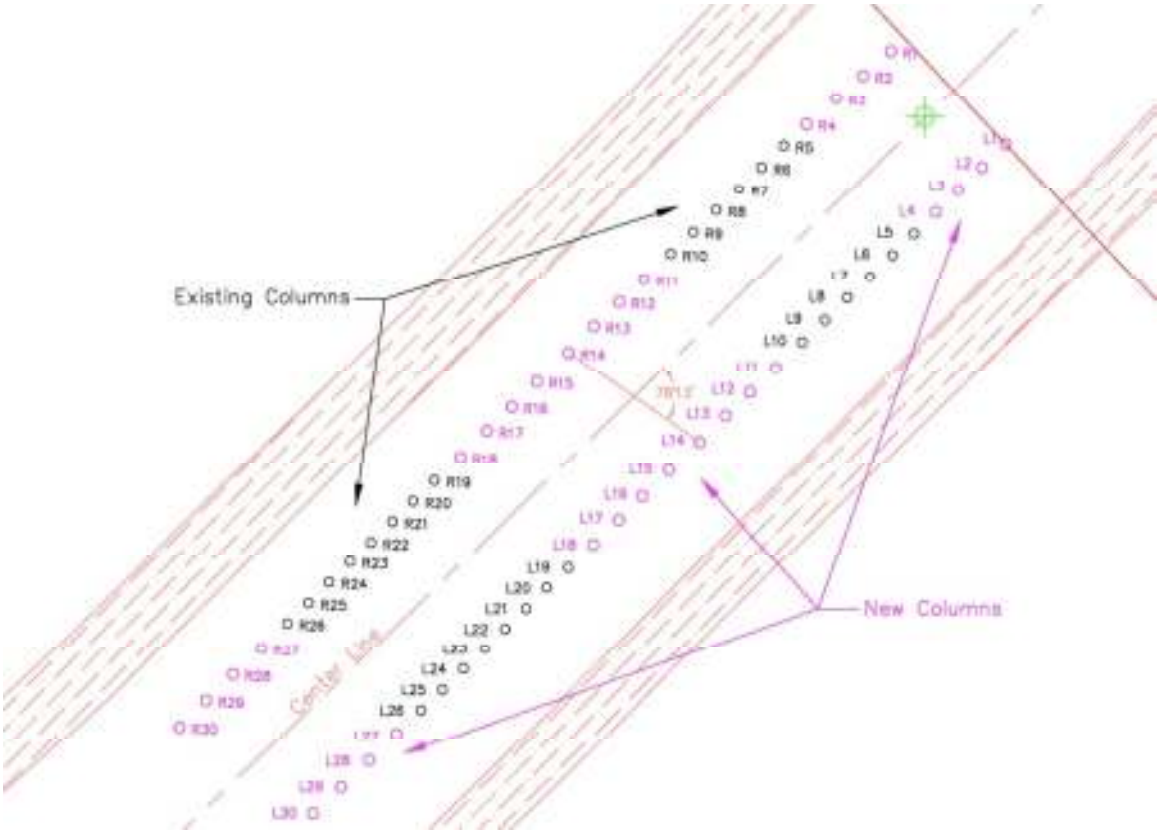

Figure A10. Column names including status as either new or original columns and a measure of asymmetry of the two rows of columns.

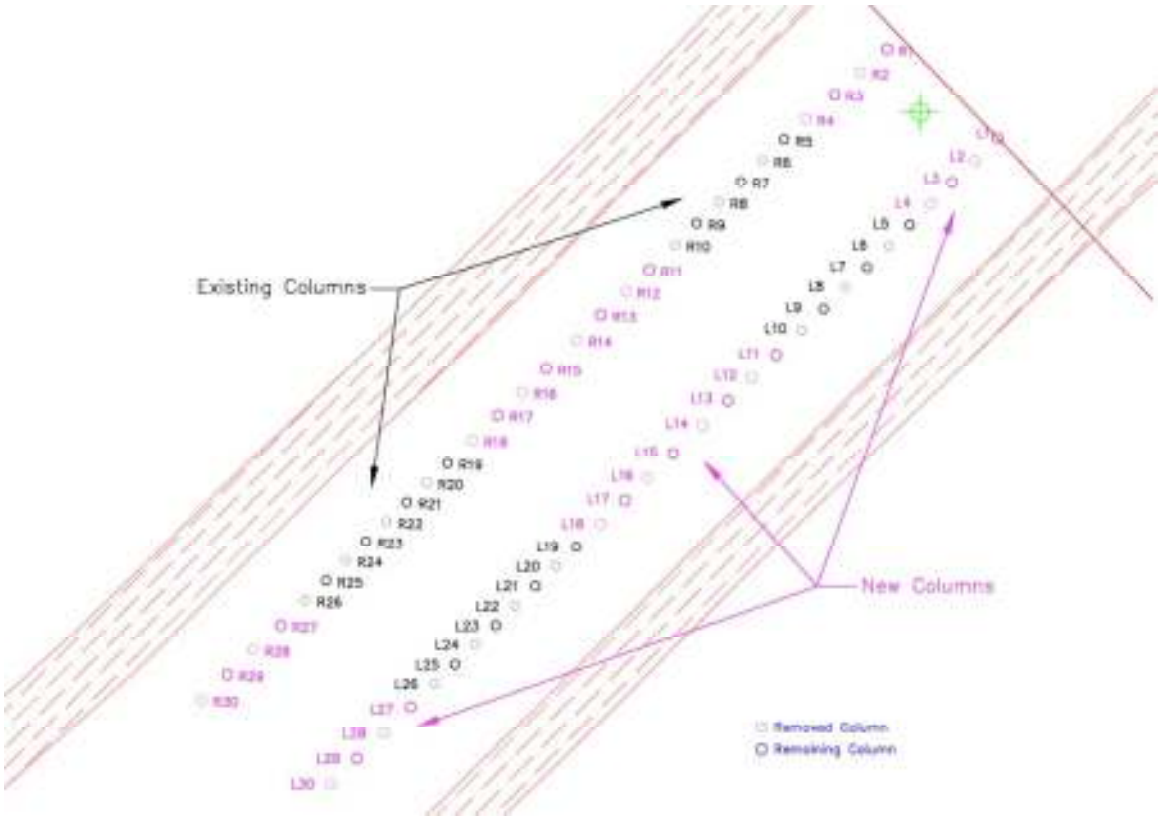

Figure A11. Every other column removed configuration showing removed and remaining columns from the original configuration.

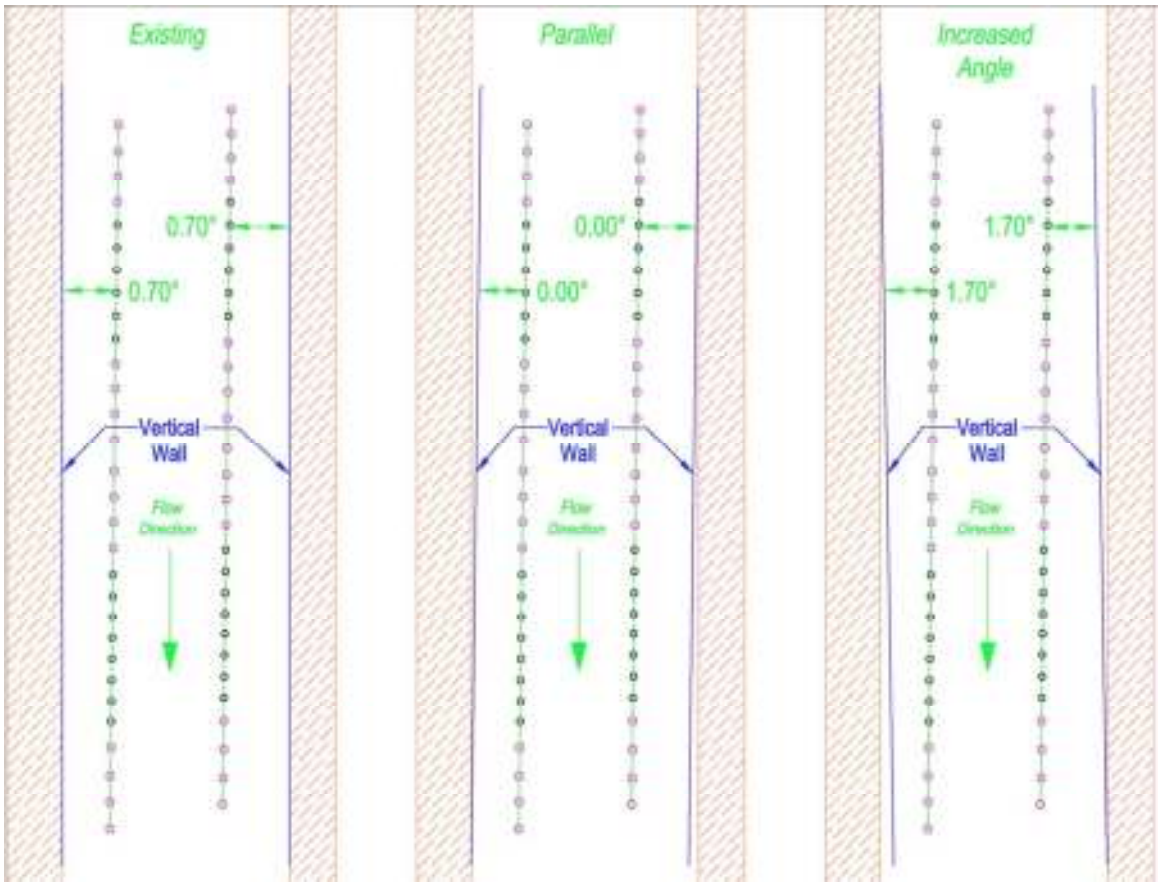

Figure A12. Changes of angle from vertical wall to column for the original configuration, zero degree/parallel configuration, and increased angle configuration.

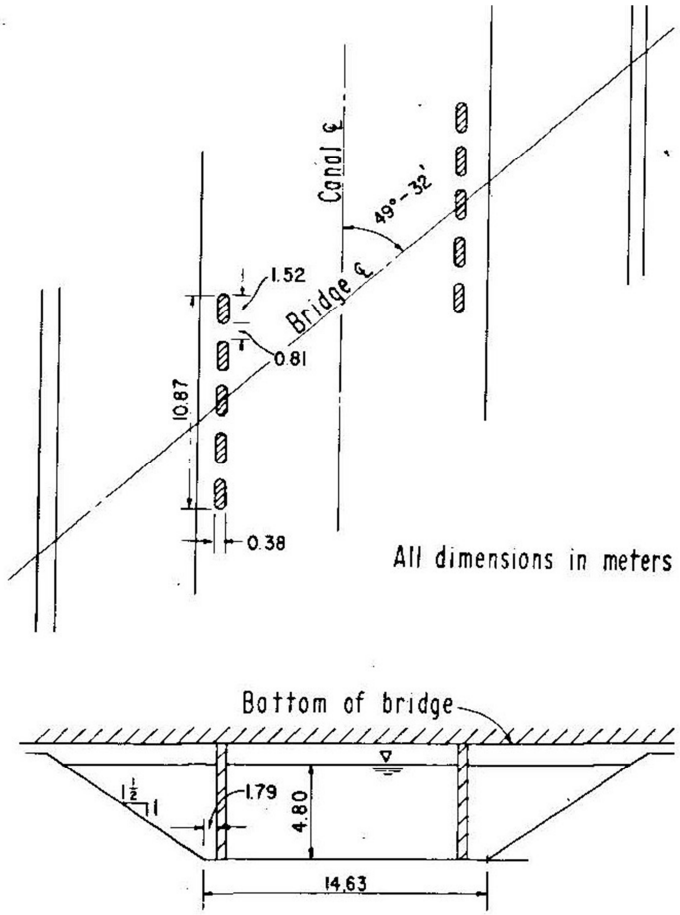

Figure A13. Plan and end views of the Delta Mendota Canal (Falvey 1980).

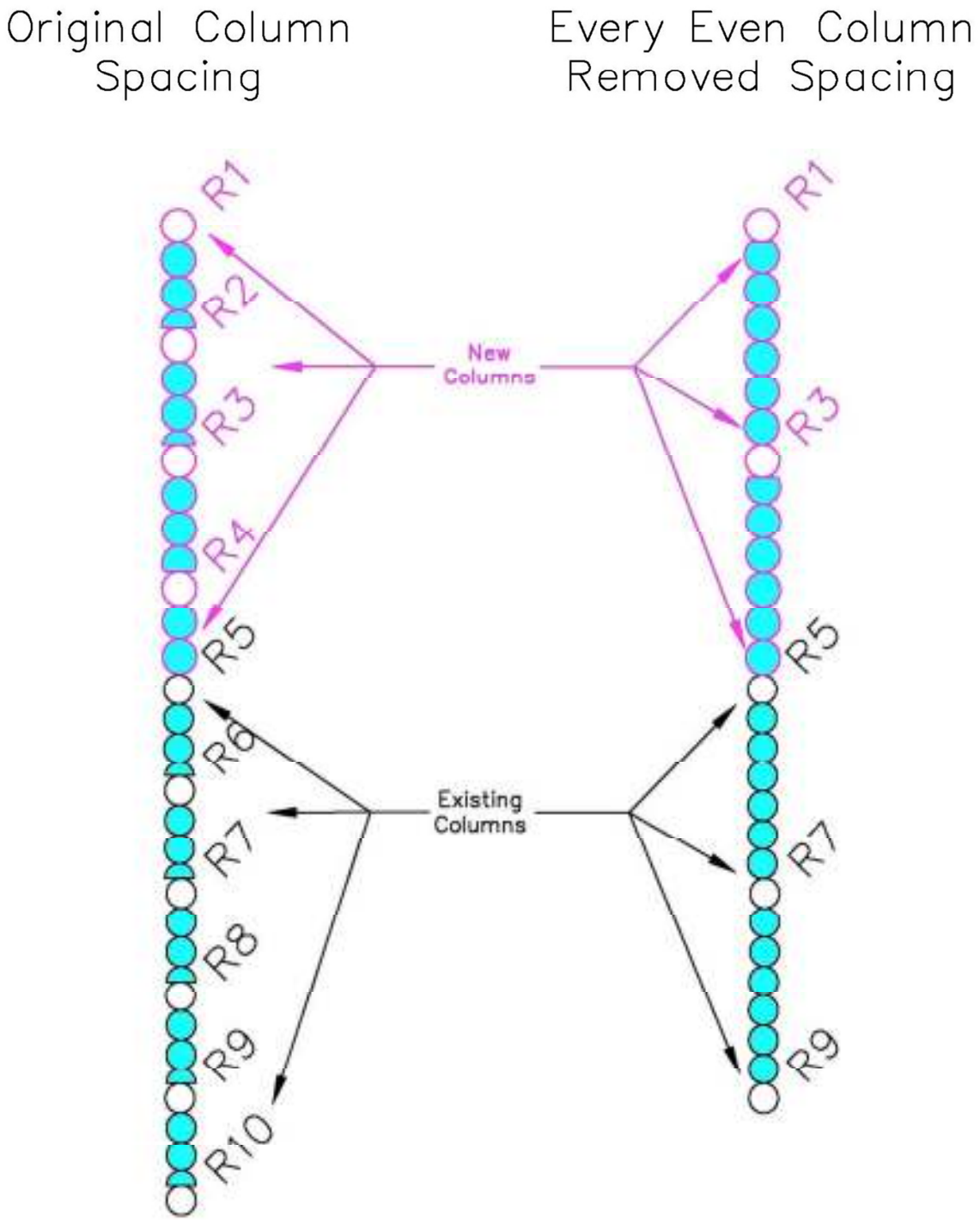

Figure A14. Space between the columns, expressed in column diameters, for each column spacing tested.

Appendix B: Data Collection

Table B1. Vertical wall configuration without approach walls compared to unmodified data from Rahmeyer et al. (2010)

All data are in model dimensions unless otherwise specified		2450 cfs		2300 cfs		2150 cfs		2000 cfs higher velocity		2000 cfs		2000 cfs Lower Velocity		1850 cfs	
1/6-10/2011		Unmodified	Vert. Wall	Unmodified	Vert. Wall	Unmodified	Vert. Wall	Unmodified	Vert. Wall	Unmodified	Vert. Wall	Unmodified	Vert. Wall	Unmodified	Vert. Wall
Flow **(Prototype cfs)**		2448	2451	2306	2305	2156	2157	2066	2072	2012	2012	1919	1922	1855	1855
mA		13.83	13.85	12.72	12.71	11.62	11.62	11	11.04	10.64	10.64	10.04	10.06	9.64	9.64
span		25	25	25	25	25	25	25	25	25	25	25	25	25	25
Depth Gauge Reading (Model ft)	max/avg	2.094	2.069	2.054	2.035	2.016	1.997	1.983	1.972	1.969	1.9415	1.958	1.932	1.896	1.869
	min	2.079	2.06	2.036	2.028	1.994	1.9875	1.957	1.964	1.953	1.936	1.943	1.925	1.873	1.86
Depth (Model in)		12.5	12.432	12	12.036	11.5	11.565	11.125	11.274	10.875	10.923	10.75	10.8	10.125	10.032
Oscillation (Model seconds/cycle)		2.125	1.528	2.128	1.55	2.132	1.64	2.144	1.5	2.146	1.6	2.184	1.5	2.159	1.65
Vertical Wave (Model in)		0.5	0.125	0.375	0.125	0.75	0.0625	0.875	0.125	0.75	0.125	0.375	0.0625	0.5	0.375
Wall Wave Height (Model in)		0.75	--	0.75	--	1.25	--	1.5	--	1.25	--	0.75	--	1	--
Location of max wave (Model ft downstream from datum)		15	20	20	20	15	15	15	15	10	15	15	20	15	20
Wave extents (Model ft from datum)		20' up to end of model	Entire Model	entire model	entire model	20' up to end of model	Entire Model	entire model	entire model	entire model	entire model	15 up to end of	15 up to end of model	entire model	entire model
Average Pressure tap readings **(Prototype feet)**	upstream	2799.3	2798.95	2798.95	2798.75	2798.5	2798.4	2798.3	2798.2	2798.15	2798	2798.15	2797.85	2797.6	2797.3
	downstream	2799.2	2798.85	2798.9	2798.7	2798.4	2798.35	2798.2	2798.1	2798.05	2797.85	2798.05	2797.8	2797.5	2797.2
	1,2,3	2799.35	2799.1	2799	2798.8	2798.6	2798.4	2798.3	2798.2	2798.2	2797.95	2798.2	2797.85	2797.6	2797.3
	4,5,6	2799.3	2799	2798.95	2798.7	2798.5	2798.4	2798.25	2798.2	2798.15	2797.95	2798.1	2797.8	2797.55	2797.25
	7,8,9	2799.25	2798.9	2798.9	2798.7	2798.45	2798.35	2798.2	2798.1	2798.1	2797.85	2798.05	2797.75	2797.5	2797.2
stop log configuration (Model in)	left	9.25	9	7.5	9	7.5	7.5	7.5	7.5	7.5	9	7.5	9	7.5	7.5
	center	9.5	8	9.5	8	9.25	8	9.25	8	9.25	7.25	9.25	7.25	7	7.25
	right	9	9.25	9	9.25	8	9.25	7	8.5	7	8.5	7	8.5	8	7
Date collected		27-Oct-10	6-Jan-11	27-Oct-10	7-Jan-11	27-Oct-10	7-Jan-11	27-Oct-10	7-Jan-11	27-Oct-10	7-Jan-11	27-Oct-10	7-Jan-11	27-Oct-10	7-Jan-11
Prototype Equivalents	Depth (Prototype ft)	9.38	9.32	9.00	9.03	8.63	8.67	8.34	8.46	8.16	8.19	8.06	8.10	7.59	7.52
	Wave Height (Prototype ft)	0.4	0.1	0.3	0.1	0.6	0.05	0.7	0.1	0.6	0.1	0.3	0.0	0.4	0.3
	Osc. Freq. (Prototype sec/cycle)	6.3750	4.5840	6.3840	4.6500	6.3960	4.9200	6.4320	4.5000	6.4380	4.8000	6.5520	4.5000	6.4770	4.9500
	Flow Rate (Prototype cfs)	2448	2451	2306	2305	2156	2157	2066	2072	2012	2012	1919	1922	1855	1855

Table B2. Vertical wall configuration without approach walls compared to unmodified data from Rahmeyer et al. (2010)

All data are in model dimensions unless otherwise specified		1700 cfs		1550 cfs		1400 cfs		1250 cfs		1100 cfs		950 cfs	
1/6-10/2011		Unmodified	Vert. Wall	Unmodified	Vert. Wall	Unmodified	Vert. Wall	Unmodified	Vert. Wall	Unmodified	Vert. Wall	Unmodified	Vert. Wall
Flow **(Prototype cfs)**		1704	1706	1552	1560	1412	1416	1245	1242	1096	1096	947	947
mA		8.76	8.77	7.95	7.99	7.27	7.29	6.54	6.53	5.97	5.97	5.47	5.47
span		25	25	25	25	25	25	25	25	25	25	25	25
Depth Gauge Reading (Model ft)	max/avg	1.834	1.812	1.778	1.753	1.755	1.732	1.708	1.678	1.647	1.64	1.597	1.578
	min	1.816	1.82	1.768	1.745	1.749	1.729	1.693	1.675	1.633	1.6365	1.583	1.5745
Depth (Model in)		9.375	9.45	8.75	8.646	8.5	8.424	7.75	7.776	7.125	7.317	6.5	6.573
Oscillation (Model seconds/cycle)		2.169	1.65	2.219	1.73	2.184	1.75	2.288	1.84	2.287	1.8	2.4	1.9
Vertical Wave (Model in)		0.25	0.125	0.1875	0.25	0.03125	0.0625	0.125	0.0625	0.125	0.0625	0.125	0.0625
Wall Wave Height (Model in)		0.625	--	0.375	--	0.0625	--	0.25	--	0.25	--	0.25	--
Location of max wave (Model ft downstream from datum)		10	10	15	20	10	20	5	20	5	5	5	20
Wave extents (Model ft from datum)		30 up to end of	Entire Model	20 up to 45 down	Entire Model	20 up to 40 down	Whole Vert. Section	20 up to 40 down	Vert. Section	20 up to 40 down	Whole Vertical Section	10 up to 35 down	Whole Vert. Section
Average Pressure tap readings **(Prototype feet)**	upstream	2797.05	2796.7	2796.6	2796.35	2796.4	2796.1	2795.85	2795.6	2795.35	2795.3	2794.9	2794.75
	downstream	2796.9	2796.6	2796.45	2796.25	2796.3	2796	2795.8	2795.5	2795.25	2795.2	2794.8	2794.65
	1,2,3	2797.1	2796.85	2796.6	2796.3	2796.4	2796.1	2795.85	2795.6	2795.35	2795.3	2794.9	2794.75
	4,5,6	2797	2796.8	2796.55	2796.25	2796.35	2796.05	2795.8	2795.55	2795.35	2795.3	2794.85	2794.7
	7,8,9	2796.9	2796.7	2795.5	2796.2	2796.3	2796	2795.8	2795.5	2795.3	2795.2	2794.8	2794.65
stop log configuration (Model in)	left	6	5	7.5	5	7.5	5	4.75	5	5.5	4	6.5	4
	center	7.25	7.25	6	6	6	6	6	6	6	6	5.25	5.25
	right	7	6.75	7	6.75	7	6.75	7	5.5	5.5	5.5	5.25	5.5
Date collected		1-Nov-10	7-Jan-11	1-Nov-10	7-Jan-11	1-Nov-10	7-Jan-11	1-Nov-10	7-Jan-11	1-Nov-10	10-Jan-11	1-Nov-10	10-Jan-11
Prototype Equivalents	Depth (Prototype ft)	7.03	7.09	6.56	6.48	6.38	6.32	5.81	5.83	5.34	5.49	4.88	4.93
	Wave Height (Prototype ft)	0.2	0.1	0.1	0.2	0.0	0.0	0.1	0.0	0.1	0.05	0.1	0.0
	Osc. Freq. (Prototype sec/cycle)	6.5070	4.9500	6.6570	5.1900	6.5520	5.2500	6.8640	5.5200	6.8610	5.4000	7.2000	5.7000
	Flow Rate (Prototype cfs)	1704	1706	1552	1560	1412	1416	1245	1242	1096	1096	947	947

Table B3. Vertical wall configuration without approach walls' velocity profile comparison with Rahmeyer et al.'s velocity profile

Velocities at 2000 cfs run (ft/s) taken at a depth of 10.875 Model in. (Rahmeyer et al. 2010)

	US		
Unmodified	left	center	right
0.75 Depth	1.19	1.14	1.13
0.50 Depth	1.19	1.18	1.16
0.25 Depth	1.09	1.13	1.07
Average	**1.16**	**1.15**	**1.12**

	DS		
Modified	left	center	right
0.75 Depth	1.16	1.08	1.08
0.50 Depth	1.19	1.16	1.17
0.25 Depth	1.06	1.1	1.13
Average	**1.14**	**1.11**	**1.13**

Taken 1/7/2011 at a Depth of 10.923 Model in

	US		
Vert. Wall	left	center	right
0.75 Depth	1.07	1.3	1.32
0.50 Depth	1.05	1.17	1.27
0.25 Depth	0.96	1.03	1.16
Average	**1.03**	**1.17**	**1.25**

	DS		
Vert. Wall	left	center	right
0.75 Depth	1.13	1.33	1.29
0.50 Depth	1.16	1.36	1.24
0.25 Depth	1.1	1.35	1.21
Average	**1.13**	**1.35**	**1.25**

Taken 1/6/2011 at a Depth of 11.2 Model in

	US		
Vert. Wall	left	center	right
top	1.04	1.22	1.32
middle	1.02	1.13	1.25
bottom	0.9	0.92	1.13
Average	**0.99**	**1.09**	**1.23**

	DS		
Vert. Wall	left	center	right
top	1.18	1.24	1.24
middle	1.12	1.31	1.19
bottom	1.05	1.25	1.15
Average	**1.12**	**1.27**	**1.19**

Table B4. Vertical wall configuration with approach walls worst case test

Depth (in)
11

Vertical Walls With Approach Walls

1/13-19/2011

Goal Flow Prototype (cfs)	Act. Flow Prototype (cfs)	Max. Gague (ft)	Min. Gague (ft)	Ave. Depth (ft)	Ave. Depth (in_{model})	Oscillation (Y/N)		Location of Max Oscillation (ft from datum)	Amplitude of Max Oscillation (in)	Frequency (sec/cycle)
						Left	Right			
1800	1798	1.945	1.939	0.913	10.96	Y	Y	20	0.19	1.60
1900	1900	1.958	1.945	0.923	11.07	Y	Y	15	0.19	1.60
2000	2003	1.949	1.923	0.907	10.89	Y	Y	15	0.50	1.60
2100	2100	1.958	1.909	0.905	10.86	Y	Y	10	1.31	1.65
2200	2202	1.983	1.928	0.927	11.12	Y	Y	10	1.19	1.62
2300	2303	1.971	1.907	0.910	10.92	Y	Y	10	1.38	1.64
2400	2403	1.985	1.923	0.926	11.11	Y	Y	10	1.38	1.63
2500	2500	1.955	1.926	0.912	10.94	Y	Y	10	0.81	1.66
2600	2603	1.962	1.932	0.919	11.02	Y	Y	Occational Waves Propogating US		

	Velocity Profile at 2000 Prototype cfs							
		US				DS		
V (fps)	FL	L	C	R	FR	L	C	R
0.75y		1.11	1.41	1.4		1.24	1.45	1.37
0.5y	0.1	1.07	1.31	1.35	-0.03	1.26	1.51	1.35
0.25y		0.91	1.03	1.25		1.18	1.57	1.31
Average		**1.03**	**1.25**	**1.33**		**1.23**	**1.51**	**1.34**

Table B5. Vertical wall configuration with approach walls worst case test

Depth (in)
12

Vertical Walls With Approach Walls

1/13-19/2011

Goal Flow Prototype (cfs)	Act. Flow Prototype (cfs)	Max. Gague (ft)	Min. Gague (ft)	Ave. Depth (ft)	Ave. Depth (in_{model})	Oscillation (Y/N)		Location of Max Oscillation (ft from datum)	Amplitude of Max Oscillation (in)	Frequency (sec/cycle)
						Left	Right			
1800	1805	2.028	2.014	0.992	11.91	Y	Y	5	0.19	1.55
1900	1900	2.045	2.030	1.009	12.11	Y	Y	10	0.25	1.50
2000	2002	2.035	2.021	1.000	11.99	Y	Y	10	0.13	1.60
2100	2104	2.029	2.010	0.991	11.89	Y	Y	20	0.25	1.60
2200	2198	2.042	2.027	1.006	12.07	Y	Y	10	0.38	1.62
2300	2305	2.051	2.005	0.999	11.99	Y	Y	5	0.88	1.60
2400	2404	2.048	2.014	1.003	12.03	Y	Y	10	1.25	1.58
2500	2503	2.085	2.020	1.024	12.29	Y	Y	5	1.38	1.57
2600	2602	2.056	1.990	0.995	11.93	Y	Y	10	1.44	1.60
2700	2700	2.035	1.978	0.978	11.74	Y	Y	10	1.25	1.60
2800	2799	2.040	1.991	0.987	11.84	Y	Y	10	1.00	1.60
3150	3145	2.045	2.032	1.010	12.12	N	N	--	--	--

	Velocity Profile at 2000 Prototype cfs							
		US				DS		
V (fps)	FL	L	C	R	FR	L	C	R
0.75y		1	1.27	1.21		1.1	1.32	1.26
0.5y	0.07	0.96	1.18	1.18	-0.01	1.03	1.35	1.2
0.25y		0.86	0.99	1.05		1.05	1.32	1.15
Average		**0.94**	**1.15**	**1.15**		**1.06**	**1.33**	**1.20**

Table B6. Vertical wall configuration with approach walls worst case test

Depth (in)
13

1/13-19/2011

Vertical Walls With Approach Walls

Goal Flow Prototype (cfs)	Act. Flow Prototype (cfs)	Ave. Depth (ft)	Ave. Depth (in_{model})	Oscillation (Y/N)		Location of Max Oscillation (ft from datum)	Amplitude of Max Oscillation (in)	Frequency (sec/cycle)
				Left	Right			
1800	1800	1.083	13.0	Y	Y	5	0.06	1.60
1900	1902	1.083	13.0	Y	Y	10	0.13	1.50
2000	2002	1.083	13.0	Y	Y	5	0.13	1.50
2100	2103	1.083	13.0	Y	Y	20	0.19	1.50
2200	2200	1.083	13.0	Y	Y	10	0.19	1.50
2300	2302	1.083	13.0	Y	Y	15	0.19	1.50
2400	2402	1.083	13.0	Y	Y	15	0.38	1.50
2500	2501	1.083	13.0	Y	Y	10	0.75	1.55
2600	2602	1.083	13.0	Y	Y	5	1.38	1.56
2700	2704	1.083	13.0	Y	Y	5	1.63	1.50
2800	2803	1.083	13.0	Y	Y	10	1.75	1.56
2900	2902	1.083	13.0	Y	Y	5	1.81	1.55
3000	3005	1.083	13.0	Y	Y	10	1.88	1.57
3100	3101	1.083	13.0	Y	Y	10	1.63	1.54
3150	3146	1.083	13.0	Y	Y	10	1.50	1.54

*Note: On the 13 inch runs for flow rates 1800-2300 cfs it seemed as though the oscillations wanted to start and would begin to occur then they would dampen out after about 5 oscillations. This would repeat ever 20-30

	Velocity Profile at 2000 Prototype cfs							
	US					DS		
V (fps)	FL	L	C	R	FR	L	C	R
0.75y		0.83	1.12	1.12		1.10	1.20	1.10
0.5y	0.02	0.88	1.03	1.09	-0.02	1.05	1.26	1.07
0.25y		0.70	0.87	0.93		0.98	1.18	1.02
Average		**0.80**	**1.01**	**1.05**		**1.04**	**1.21**	**1.06**

Table B7. Vertical wall configuration without approach walls comparison test

Depth (in)
13

1/20/2011

Goal Flow Prototype (cfs)	Act. Flow Prototype (cfs)	Ave. Depth (ft)	Ave. Depth (in_{model})	Oscillation (Y/N)		Location of Max Oscillation (ft from datum)	Amplitude of Max Oscillation (in)	Frequency (sec/cycle)
				Left	Right			
2600	2595	1.083	13.0	Y	Y	10	0.38	1.56
2700	2703	1.083	13.0	Y	Y	20	0.69	1.54
2800	2799	1.083	13.0	Y	Y	20	1.00	1.52
2900	2904	1.083	13.0	Y	Y	5	1.25	1.52
3000	3003	1.083	13.0	Y	Y	5	2.06	1.54
3100	3102	1.083	13.0	Y	Y	10	2.06	1.55
3200	3198	1.083	13.0	Y	Y	10	2.25	1.56
3300	3308	1.083	13.0	Y	Y	15	2.38	1.57
3400	3400	1.083	13.0	Y	Y	5	2.25	1.56
3500	3506	1.083	13.0	Y	Y	5	2.25	1.54
3600	3596	1.083	13.0	Y	Y	5	1.81	1.55
3700	3702	1.083	13.0	Y	Y	5	1.31	1.58
3800	3816	1.083	13.0	Y	Y	10	1.63	1.53
4000	4003	1.083	13.0	Y	Y	No Measurable Oscillations		

Without Nose Cones								
3300	3297	1.083	13.0	Y	Y	5	2.25	1.53
With Nose Cones								
3300	3297	1.083	13.0	N	N	No Measurable Oscillations		

Velocity Profile at 2000 Prototype cfs Without Nose Cones

	US					DS		
V (fps)	FL	L	C	R	FR	L	C	R
0.75y		0.89	1.12	1.11		1.04	1.19	1.12
0.5y	0.68	0.82	1.05	1.07	0.84	1.00	1.21	1.10
0.25y		0.72	0.88	0.91		0.94	1.15	1.00
Average		**0.81**	**1.02**	**1.03**		**0.99**	**1.18**	**1.07**

Table B8. Vertical walls configuration, wall to column angle of 0 degrees

Without approach walls and column to wall angle = 0 degrees

Depth (in)
13

2/10/2011

Goal Flow Prototype (cfs)	Act. Flow Prototype (cfs)	Ave. Depth (ft)	Ave. Depth (in_{model})	Oscillation (Y/N)		Location of Max Oscillation (ft from datum)	Amplitude of Max Oscillation (in)	Frequency (sec/cycle)	Recurrance Interval (s)	Oscillation Range (ft from datum)
				Left	Right					
2000	2002	1.083	13.0	Y	Y	--	--	--	--	--
2400	2416	1.083	13.0	Y	Y	10	0.13	1.48	10	All Vert
2700	26.95	1.083	13.0	Y	Y	5	0.25	1.47	20	All Vert
3000	3006	1.083	13.0	Y	Y	5	0.50	1.48	30	All Vert
3300	3305	1.083	13.0	Y	Y	10	1.00	1.50	Steady	All Vert
3500	3509	1.083	13.0	Y	Y	10	0.75	1.48	Steady	All Vert
3700	3707	1.083	13.0	Y	Y	10	0.50	1.60	Sproadic	All Vert

	Velocity Profile at 2000 Prototype cfs							
		US				DS		
V (fps)	FL	L	C	R	FR	L	C	R
0.75y		0.82	1.02	0.88		0.93	1.01	0.88
0.5y	0.95	0.84	0.94	0.83	0.72	0.89	1.09	0.90
0.25y		0.75	0.79	0.79		0.85	1.04	0.85
Average		**0.80**	**0.92**	**0.83**		**0.89**	**1.05**	**0.88**

Table B9. Vertical walls configuration, wall to column angle increased by 1 degree

Without approach walls and column to wall angle increased by 1 degree

Depth (in)
13

2/24/2011-3/1/2011

Goal Flow Prototype (cfs)	Act. Flow Prototype (cfs)	Ave. Depth (ft)	Ave. Depth (in_{model})	Oscillation (Y/N)		Location of Max Oscillation (ft from datum)	Amplitude of Max Oscillation (in)	Frequency (sec/cycle)	Recurrance Interval (s)	Oscillation Range (ft from datum)
				Left	Right					
2000	1997	1.083	13	Y	Y	--	--	--	--	--
2400	2401	1.083	13	Y	Y	15	0.25	1.48	Steady	All Vert
2700	2695	1.083	13	Y	Y	20	0.31	1.49	Steady	All Vert
3000	3012	1.083	13	Y	Y	15	1.50	1.52	Steady	All Vert
3300	3299	1.083	13	Y	Y	15	1.75	1.50	Steady	All Vert
3500	3511	1.083	13	Y	Y	15	0.81	1.51	Steady	All Vert
3700	3699	1.083	13	Y	Y	--	--	--	Occational	All Vert

	Velocity Profile at 2000 Prototype cfs							
	US					DS		
V (fps)	FL	L	C	R	FR	L	C	R
0.75y		0.99	1.06	1.00		0.97	1.15	1.00
0.5y	0.48	0.99	0.99	0.93	0.75	0.90	1.19	0.93
0.25y		0.83	0.86	0.85		0.85	1.03	0.96
Average		**0.94**	**0.97**	**0.93**		**0.91**	**1.12**	**0.96**

Table B10. Vertical walls configuration with every other column removed

Depth (in)
11

3/3-5/2011

Goal Flow Prototype (cfs)	Act. Flow Prototype (cfs)	Oscillation (Y/N)		Location of Max Oscillation (ft from datum)	Amplitude of Max Oscillation (in)	Frequency (sec/cycle)	Recurrance Interval (s)	Oscillation Range (ft from datum)
		Left	Right					
2000	2005	N	N	--	--	--	--	--
2400	2401	Y	Y	15	0.13	1.60	Steady	All Vert
2700	2705	Y	Y	10	0.31	1.63	Steady	All Vert
3000	2997	Y	Y	10	0.38	1.53	Steady	All Vert
3300	3308	N	N	Surface waves were prominent, no noticible oscillations				
3500	3496	N	N	Surface waves were prominent, no noticible oscillations				
3700	3704	N	N	Surface waves were prominent, no noticible oscillations				

	Velocity Profile at 2000 Prototype cfs and 11 7/16 Model Inch Depth							
	US					DS		
V (fps)	FL	L	C	R	FR	L	C	R
0.75y		1.03	1.25	1.06		1.06	1.25	1.1
0.5y	0.66	0.91	1.18	1.00	1.00	1.05	1.28	1.03
0.25y		0.92	0.98	0.90		0.96	1.16	1.02
Average		**0.95**	**1.14**	**0.99**		**1.02**	**1.23**	**1.05**

Table B11. Vertical walls configuration with every other column removed

Depth (in)
12

3/3-5/2011

Goal Flow Prototype (cfs)	Act. Flow Prototype (cfs)	Oscillation (Y/N)		Location of Max Oscillation (ft from datum)	Amplitude of Max Oscillation (in)	Frequency (sec/cycle)	Recurrance Interval (s)	Oscillation Range (ft from datum)
		Left	Right					
2000	2005	N	N	--	--	--	--	--
2400	2401	Y	Y	15	0.13	1.60	Steady	All Vert
2700	2702	Y	Y	10	0.25	1.55	Steady	All Vert
3000	3000	Y	Y	15	0.44	1.58	Steady	All Vert
3300	3308	Y	Y	10	0.44	1.53	Steady	All Vert
3500	3496	N	N	Surface waves were prominent, no noticible oscillations				
3700	3704	N	N	Surface waves were prominent, no noticible oscillations				

	Velocity Profile at 2000 Prototype cfs and 12 Model Inch Depth							
	US					DS		
V (fps)	FL	L	C	R	FR	L	C	R
0.75y		0.90	1.13	0.99		1.01	1.12	1.02
0.5y	0.71	0.86	1.07	0.95	0.98	0.99	1.13	1.02
0.25y		0.71	0.90	0.88		0.90	1.10	0.95
Average		**0.82**	**1.03**	**0.94**		**0.97**	**1.12**	**1.00**

Table B12. Vertical walls configuration with every other column removed

Depth (in)
13

3/3-5/2011

Goal Flow Prototype (cfs)	Act. Flow Prototype (cfs)	Oscillation (Y/N)		Location of Max Oscillation (ft from datum)	Amplitude of Max Oscillation (in)	Frequency (sec/cycle)	Recurrance Interval (s)	Oscillation Range (ft from datum)
		Left	Right					
2000	2005	N	N	--	Inmeasurable	1.50	Steady	All Vert
2400	2401	Y	Y	15	0.13	1.65	Steady	All Vert
2700	2702	Y	Y	10	0.13	1.67	Steady	All Vert
3000	3003	Y	Y	15	0.25	1.51	Steady	All Vert
3300	3308	Y	Y	10	0.38	1.58	Steady	All Vert
3500	3496	Y	Y	10	0.50	1.50	Steady	All Vert
3700	3704	N	N	Surface waves were prominent, no noticible oscillations				

	Velocity Profile at 2000 Prototype cfs and 13 3/16 Model Inch Depth							
	US					DS		
V (fps)	FL	L	C	R	FR	L	C	R
0.75y		0.90	0.99	0.88		0.88	1.00	0.94
0.5y	0.65	0.82	0.88	0.83	0.85	0.89	1.05	0.88
0.25y		0.72	0.77	0.77		0.81	0.96	0.86
Average		**0.81**	**0.88**	**0.83**		**0.86**	**1.00**	**0.89**

Table B13. Mean velocity calculations for the vertical walls with approach walls configuration assuming a rectangular cross section

Depth	11	model in
Base Width	92.0	model in
Area	7.03	model ft^2

Flow Rate (Prototype cfs)	Flow Rate (Model cfs)	US Velocity (Model fps)
1800	7.41	1.05
1900	7.82	1.11
2000	8.23	1.17
2100	8.64	1.23
2200	9.05	1.29
2300	9.47	1.35
2400	9.88	1.41
2500	10.29	1.46
2600	10.70	1.52
2700	11.11	1.58
2800	11.52	1.64
2900	11.93	1.70
3000	12.35	1.76
3100	12.76	1.82
3150	12.96	1.84

Depth	12	model in
Base Width	92.0	model in
Area	7.67	model ft^2

Flow Rate (Prototype cfs)	Flow Rate (Model cfs)	US Velocity (Model fps)
1800	7.41	0.97
1900	7.82	1.02
2000	8.23	1.07
2100	8.64	1.13
2200	9.05	1.18
2300	9.47	1.23
2400	9.88	1.29
2500	10.29	1.34
2600	10.70	1.40
2700	11.11	1.45
2800	11.52	1.50
2900	11.93	1.56
3000	12.35	1.61
3100	12.76	1.66
3150	12.96	1.69

Depth	13	model in
Base Width	92.0	model in
Area	8.31	model ft^2

Flow Rate (Prototype cfs)	Flow Rate (Model cfs)	US Velocity (Model fps)
1800	7.41	0.89
1900	7.82	0.94
2000	8.23	0.99
2100	8.64	1.04
2200	9.05	1.09
2300	9.47	1.14
2400	9.88	1.19
2500	10.29	1.24
2600	10.70	1.29
2700	11.11	1.34
2800	11.52	1.39
2900	11.93	1.44
3000	12.35	1.49
3100	12.76	1.54
3150	12.96	1.56

Table B14. Mean velocity calculations for the vertical walls without approach walls assuming a trapezoidal cross section

Depth	13	model in
Base Width	92.0	model in
m_{Left}	1.47	
m_{Right}	1.39	
Area	9.98	model ft^2

Flow Rate (Prototype cfs)	Flow Rate (Model cfs)	US Velocity (Model fps)
2600	10.70	1.07
2700	11.11	1.11
2800	11.52	1.15
2900	11.93	1.20
3000	12.35	1.24
3100	12.76	1.28
3200	13.17	1.32
3300	13.58	1.36
3400	13.99	1.40
3500	14.40	1.44
3600	14.81	1.48
3700	15.23	1.53
3800	15.64	1.57
4000	16.46	1.65

Table B15. Original column configuration in trapezoidal canal

3/10/2011 Existing Configuration

Goal Flow (Prototype cfs)	Act. Flow (Prototype cfs)	Depth (Model in.)	Oscillation (Y/N)		Location of max oscillation (ft from Datum)	Vertical Wave Height (Model in)	Wall Wave Height (Model in)	Frequency (Model Sec/Cycle)	Oscillation Range (Model ft. from Datum)	Column R1 Frequency (Model Sec/Cycle)	Column R2 Frequency (Model Sec/Cycle)	Column R3 Frequency (Model Sec/Cycle)	R1 Frequency Ratio	R2 Frequency Ratio	R3 Frequency Ratio
2000	2012	10.875	Y	Y	10	0.75	1.25	2.146	Entire Model	--	--	--	--	--	--
2000	2006	10.875	Y	Y	15	0.75	1.38	2.109	Entire Model	Unmeasurable	2.167	1.96	--	1.03	0.93
2300	2306	12	Y	Y	20	0.38	0.75	2.128	Entire Model	--	--	--	--	--	--
2300	2303	11.75	Y	Y	15	0.75	1.38	2.147	Entire Model	Unmeasurable	1.9	1.9	--	0.88	0.88
2300	2305	12.25	Y	Y	15	0.50	1.00	2.11	Entire Model	Unmeasurable	2.191	2.1	--	1.04	1.00
2450	2448	12.5	Y	Y	15	0.50	0.75	2.125	Entire Model	--	--	--	--	--	--
2450	2456	12.375	Y	Y	15	0.25	0.50	2.122	Entire Model	Unmeasurable	2.1	2.1	--	0.99	0.99
3000	3013	13	N	N	Wavy WS					--	--	--	--	--	--

Table B16. Every other column removed configuration in trapezoidal canal

3/7-8/2011 Every Other Column Removed

Goal Flow (Prototype cfs)	Act. Flow (Prototype cfs)	Depth (Model in.)	Oscillation (Y/N)		Location of max oscillation (ft from Datum)	Vertical Wave Height (Model in)	Wall Wave Height (Model in)	Frequency (Model Sec/Cycle)	Oscillation Range (Model ft. from Datum)	Column R1 Frequency (Model Sec/Cycle)	Column R3 Frequency (Model Sec/Cycle)	Column R5 Frequency (Model Sec/Cycle)	R1 Frequency Ratio	R3 Frequency Ratio	R5 Frequency Ratio
2000	2003	10.875	Y	Y	5	0.06	0.19	2.191	All Column Sect.	--	--	--	--	--	--
2000	1999	10.875	Y	Y	15	0.06	0.19	2.156	All Column Sect.	Unmeasurable	2.091	2.034	--	0.97	0.94
2300	2295	12	Y	Y	15	0.13	0.25	2.167	Datum to End	--	--	--	--	--	--
2300	2303	11.75	Y	Y	15	0.13	0.25	2.159	Datum to End	Unmeasurable	2.06	2.016	--	0.95	0.93
2450	2457	12.5	Y	Y	15	0.06	0.38	2.103	Datum to End	--	--	--	--	--	--
2450	2448	12.25	Y	Y	15	0.06	0.19	2.129	Datum to End	Unmeasurable	2.038	2.072	--	0.96	0.97
3000	3000	13	Y	Y	15	0.13	0.38	1.3	All Column Sect.	--	--	--	--	--	--